PROCEEDINGS OF SPIE

SPIEDigitalLibrary.org/conference-proceedings-of-spie

Characterization of low-mass deformable mirrors and ASIC drivers for high-contrast imaging

Camilo Mejia Prada, Li Yao, Yuqian Wu, Lewis C. Roberts, Chris Shelton, et al.

SPIE.

Downloaded From: https://www.spiedigitallibrary.org/conference-proceedings-of-spie on 10/6/2017 Terms of Use: https://spiedigitallibrary.spie.org/ss/TermsOfUse.aspx

Characterization of Low Mass Deformable Mirrors and ASIC drivers for high-contrast imaging

Camilo Mejia Prada[a], Li Yao[b], Yuqian Wu[b], Lewis C. Roberts, Jr.[a], Chris Shelton[a], and Xingtao Wu[b]

[a]Jet Propulsion Laboratory, California Institute of Technology, Pasadena, CA, USA;
[b]Microscale, Inc., Woburn, MA, USA

ABSTRACT

The development of compact, high performance Deformable Mirrors (DMs) is one of the most important technological challenges for high-contrast imaging on space missions. Microscale Inc. has fabricated and characterized piezoelectric stack actuator deformable mirrors (PZT-DMs) and Application-Specific Integrated Circuit (ASIC) drivers for direct integration. The DM-ASIC system is designed to eliminate almost all cables, enabling a very compact optical system with low mass and low power consumption. We report on the optical tests used to evaluate the performance of the DM and ASIC units. We also compare the results to the requirements for space-based high-contrast imaging of exoplanets.

Keywords: Deformable mirrors, wavefront control, high-contrast imaging

1. INTRODUCTION

Direct imaging of Earth-like planets requires techniques and instruments for light suppression, such as wavefront control and coronagraphs, with precision that can only be achieved through the use of deformable mirrors[1,2]. On ground-based systems, DMs are used to correct for turbulences in Earth's atmosphere in addition to static aberrations in the optics.[3] On space-based applications, DMs are used to correct for slowly time varying aberrations from thermal misalignments, but require very high accuracy, stability, low power consumption and low mass.[4]

A major problem with current high-actuator-count DM drivers is the number of connections and cables, in addition to the mass of the electronics.[5] The cables are arranged in bundles, which are expensive to manufacture and have considerable mass and complexity. Figure (1a) shows two deformable mirrors connected at the High Contrast Image Testbed chamber at the Jet Propulsion Laboratory. The fat cable bundles shown in Figure (1a) demonstrate these issues, where the electronics display thousand of wires/connections.

An Application-Specific Integrated Circuit (ASIC) designed to control the DMs will vastly reduce the mass of the electronics and reduces the number of required wires by two orders of magnitude.[6] Figure (1b) shows a prototype ASIC-DM that aims to solve the cabling/connector challenge. This integrated ASIC-DM is ideal for space missions, where it offers significant reduction in mass, power and complexity, with performance compatible for high-contrast observations of exoplanets. In addition, only a few wires will connect it to the control computer greatly simplifying integration, reducing costs and increasing reliability. In future developments, it can be applied to other different DM formats while improving reliability.

These ASICs can also be used with active primary mirrors such as the Active Hybrid Mirrors[7] or the Active Shell Mirrors.[8] Both of these mirror concepts use segmented primary mirrors with each segment having dozens of actuators. These technologies are under consideration for the generation flagship missions: LUVOIR[9] and Far Infrared Surveyor. ASICs bonded to each segment would eliminate many cables and electronics packaging, leading to a lighter primary segment. This addresses a priority 1 technology gap in the 2016 Cosmic Origins technology report.

©2017 California Institute of Technology. Government sponsorship acknowledged.
Further author information: cprada@jpl.nasa.gov

Techniques and Instrumentation for Detection of Exoplanets VIII, edited by Stuart Shaklan, Proc. of SPIE
Vol. 10400, 1040011 · © 2017 SPIE · CCC code: 0277-786X/17/$18 · doi: 10.1117/12.2271500

Downloaded From: https://www.spiedigitallibrary.org/conference-proceedings-of-spie on 10/6/2017 Terms of Use: https://spiedigitallibrary.spie.org/ss/TermsOfUse.aspx

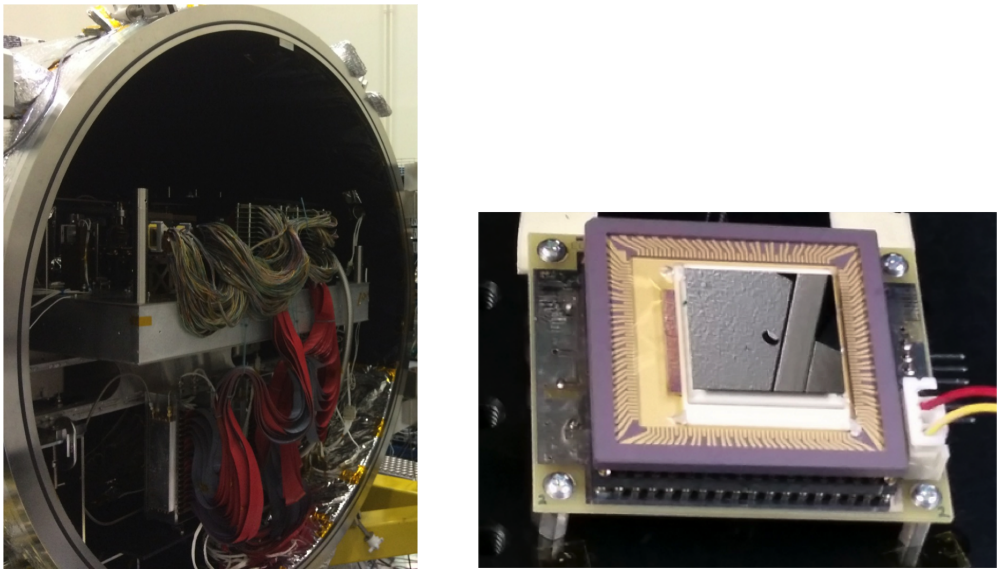

(a) (b)

Figure 1: Two deformable mirrors connected at JPL. (b) Driver ASIC for DMs.

We have successfully prototyped and tested several 4x4 DMs, a 16x16 DM and a 32x32 format Switch-Mode (SM) ASIC, which consumes only 2mW static power (total, not per-actuator). The 4x4 DMs were designed to help us carry out experiments to determine best combination of actuators and facesheet. Through this paper, we discuss the interferometric optical characterization used to evaluate the performance of the DM facesheet on a single actuators and full mirror scale.

A number of constraints were imposed on key parameters of this design, including sub-picoamp levels of leakage across turned-off switches and from switch-to-substrate, control resolution of 0.04 mV, satisfactory rise/fall times, and a near-zero on-chip crosstalk over a useful range of operating temperatures.

2. FABRICATION AND CHARACTERIZATION

2.1 PZT Deformable Mirror

The experimental characterization presented in this paper use PZT deformable mirrors designed and fabricated by Microscale, Inc. Figure (2a) shows a cross section of the DM-ASIC structure, comprising of a driver ASIC base substrate, which supports an array of piezoelectric stack actuators, both of which are bonded to a pre-structured silicon facesheet that can be as thick as a few hundred microns.

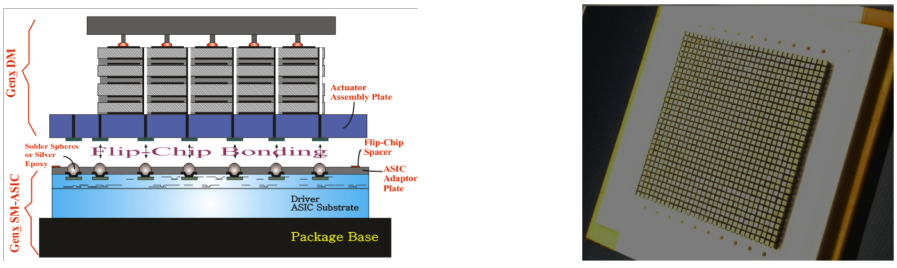

(a) (b)

Figure 2: Cross-sectional view of the DM-ASIC architecture. (b) Assembled stack actuator array without face-sheet.

To achieve high DM actuator yield, we assembled piezoelectric stack actuators in an array (Figure (2b)). This approach allows inspection of the actuators before they are assembled, plus a post-assembly inspection

Downloaded From: https://www.spiedigitallibrary.org/conference-proceedings-of-spie on 10/6/2017 Terms of Use: https://spiedigitallibrary.spie.org/ss/TermsOfUse.aspx

to ensure all actuators are performing properly. Thus 100 % yield at the actuator layer can be verified before carrying on with mirror integration. The facesheet is manufactured from a Silicon-on-Insulator (SOI) chip, with its device-side Si (polished) as the facesheet, and the handle-side Si with posts for mechanical linkage to the actuators. Furthermore, the facesheet SOI side can be coated with any type of mirror coating. As a result, the facesheet does not suffer print-through or scalloping, and the resulting influence function is uniform.

In order to understand the interaction between the mirror and the actuators, we tested four different mirrors of 4x4 actuators and one of 16x16 actuators (Figure (3a), (3b)). Table 1 gives the specifications of the DMs.

Device	Actuator Size (mm)	Pixel pitch (mm)	Mirror/Post thickness (microns)
4x4(1)	0.9x0.9x1.5	1.8	250/550
4x4(2)	0.9x0.9x1.5	2.4	75/600
4x4(3)	0.9x0.9x1.5	2.4	125/550
4x4(4)	0.9x0.9x1.5	2.4	250/550
16x16	0.9x0.9x1.5	1.8	125/550

Table 1: DM specifications.

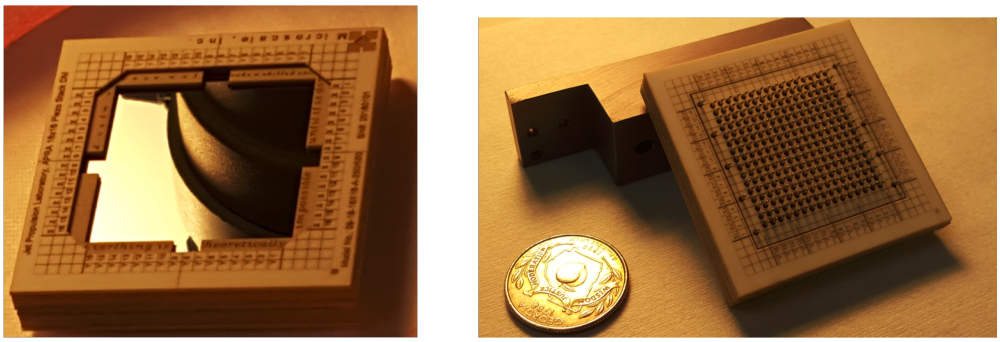

(a) (b)

Figure 3: (a) 16x16 DM front. (b) 16x16 DM back.

2.2 Surface quality

For a precise analysis of the DM's surface and performance, the primary instrument for testing was a Zygo interferometer looking face-on at the DM. Figure (4) show 2D maps of the mirror surface over the entire DM for devices (2), (3) and (4) which have the same pitch but different mirror/post thickness. A uniform voltage across all the actuators does not flatten the surface of the DM; the peak-to-valley error measured was 1.05 μm, 2.01 μm and 1.13 μm respectively.

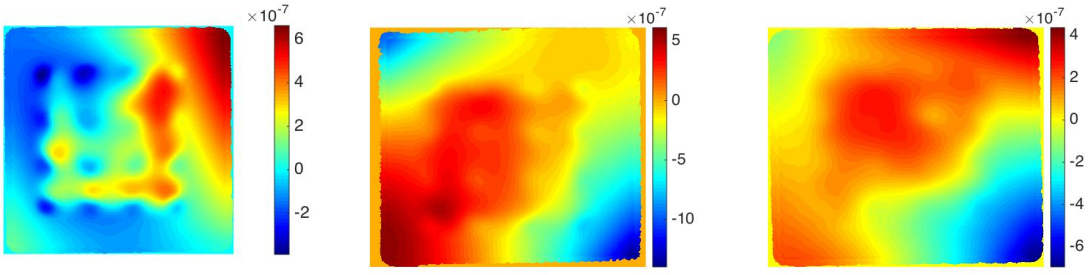

(a) (b) (c)

Figure 4: Surface profile: (a) 4x4(2), (b) 4x4(3), and (c) 4x4(4).

Downloaded From: https://www.spiedigitallibrary.org/conference-proceedings-of-spie on 10/6/2017 Terms of Use: https://spiedigitallibrary.spie.org/ss/TermsOfUse.aspx

As we can see in device (2), if the mirror thickness is too thin, the surface presents a periodic error in a square pattern with the same period as the actuator pitch. This is due to a mechanical sagging of the surface sheet on the actuator posts. On the other hand, if the mirror thickness is too thick, it becomes stiff and loses stroke, as we will discuss in the following section. Though, it also improves surface flatness measured by the change in Z4-8 Zernike coefficients which goes from $(-0.19, -0.35, 0.0031, 0.05, -0.0009)$ μm to $(-0.11, -0.15, 0.02, 0.003, 0.05)$ μm for devices (3) and (4).

2.3 Influence Function

The influence function of a DM is a 2D function that describes the spatial extent of mirror deformation for a single actuator. It includes the coupling with its neighboring actuators and the gain from different voltages. It is necessary to optimize the influence function for a DM targeting high contrast observations, but more importantly to insure that the influence function is uniform and stable across the DM.

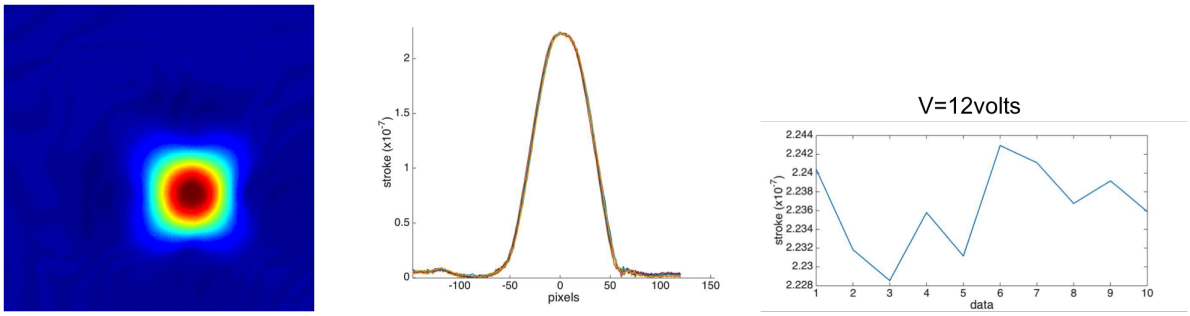

(a) (b) (c)

Figure 5: Surface: (a) Single actuator poke, (b) cross section, and (c) stability

First, we study the stability and repeatability of the actuation by grounding all the actuators except a single one, which has 12V. Figures (5a) shows a 2D map of the mirror surface where piston has been removed, in figure (5b) we superimpose a cross-section curve for 10 consecutive measurements and show the fitted peak surface displacement in figure (5c). The stability, measured as the standard deviation of the measurements, was calculated to be 1.72, 1.36, 0.47 and 1.27 μm for devices (1-4).

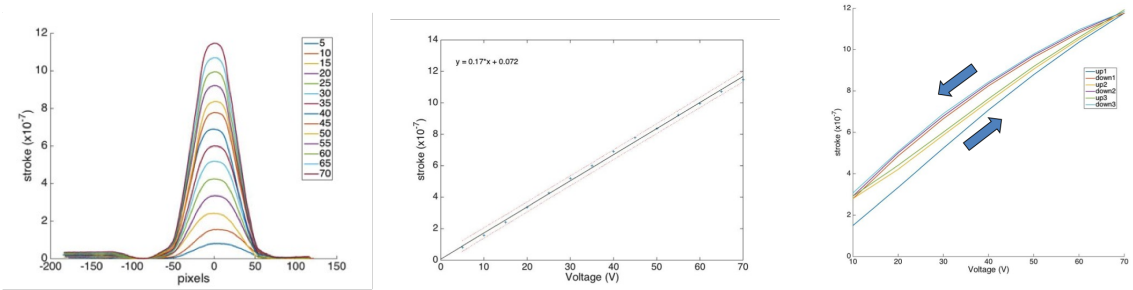

(a) (b) (c)

Figure 6: (a) Surface cross section at different voltages, (b) stroke and (c) hysteresis

The electronics used allow us to apply voltages between 0 and 100 V, but we limited the maximum voltage to 70 V for the sake of equipment safety. Figure (6a) shows the cross-section of the surface displacement at different voltages from 5 to 70 V every 5V. The fitted peak surface displacement is shown in figure (6b) where we can see a clear linear relation between voltage and stroke within the fitting error. With this stroke measurements, we calculated a gain of 12.3, 21, 17 and 12 nm/V for devices (1-4). If we actuate the mirror in a cyclic fashion, the stroke presents a typical PZT hysteresis loop as shown in figure (6c).

Next, for each of the 4x4 DMs, we studied the influence function of actuators from the center, edge and corners. Each is expected to have a different influence function because of differing mechanical support. Figure

Downloaded From: https://www.spiedigitallibrary.org/conference-proceedings-of-spie on 10/6/2017 Terms of Use: https://spiedigitallibrary.spie.org/ss/TermsOfUse.aspx

(7a) shows the X-cross section of the different influence functions. We can see that the influence functions are almost independent of the actuator position, except in the tail of the function for edge and corner actuators. We can understand this effect due to the asymmetric stress profile that the mirror surface experiences at the last actuator. On the other hand, the Y-influence function only differs in the tail for the corner actuator, as expected.

We also observed that the influence function is almost a Gaussian without full rotational symmetry but instead a more squared symmetry. To understand the influence function as a function of mirror thickness, we can parametrize the shape in a principal direction with two number as shown in figure (7c), the coupling factor and half-point. In general, we would like to have influence functions with half-point > 0.5 and coupling factors as small as possible. Table 2 summarizes the influence function parameters measured for devices (1-4), which have different mirror thickness.

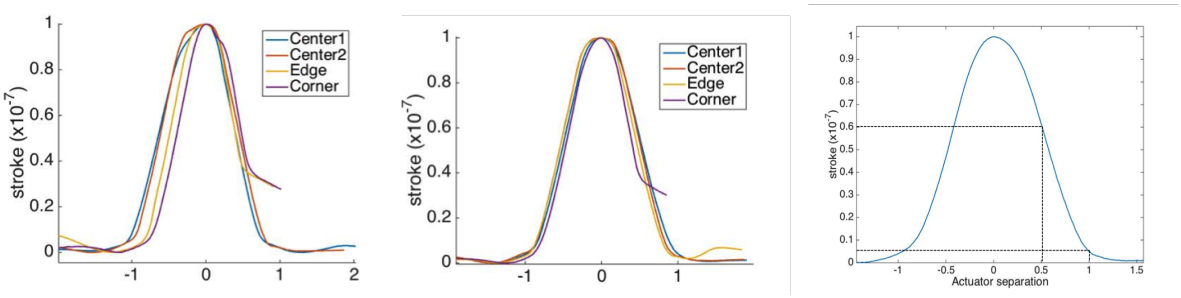

(a) (b) (c)

Figure 7: Influence function: (a) X-cross section, (b) Y-cross section, (c) coupling factor and half point.

Finally, we verified the influence function superposition on the different 4x4 DMs. We named two central actuators as B8 and T8, and an edge actuator as T5. Figure (8a) shows the influence function for B8, T8, B8 and T8, and B8+T8. Figure (8b) shows the influence function superposition for 3 actuators near an edge. Table 2 summarizes the superposition observed for devices (1-4).

Device	PV(μm)	Capacitance(nF)	Stability(nm)	Gain(nm/V)	Coupling Factor	Half Point	Superpo
4x4(1)	2.62	12.78±1.41	1.72	12	0.032	0.58	Y
4x4(2)	1.05	14.7±0.49	1.36	21	0.017	0.428	N
4x4(3)	2.01	13.21±0.61	0.47	17	0.039	0.61	Y
4x4(4)	1.13	13.55±0.81	1.27	12	0.043	0.541	Y

Table 2: Influence function parameters for 4x4 DMs.

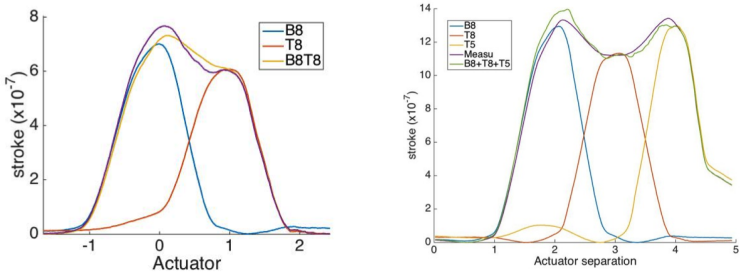

(a) (b)

Figure 8: Central actuators superposition, and (b) corner actuators superposition.

Downloaded From: https://www.spiedigitallibrary.org/conference-proceedings-of-spie on 10/6/2017 Terms of Use: https://spiedigitallibrary.spie.org/ss/TermsOfUse.aspx

3. CONCLUSIONS

We have studied the influence function of PZT deformable mirrors designed and fabricated by Microscale, using a Zygo interferometer looking face-on at the DM. We conclude that influence function is almost independent of the actuator position, except in the tail of the function for edge and corner actuators due to the asymmetric stress profile.

The thickness of the mirror has a very important role in the DM design. In device (2), if the mirror thickness is too thin, the surface presents a periodic surface error due to sagging. It also produces an influence function that does not follow superposition, which we can understand by the fact that its half point is < 0.5. On the other hand, it has the larges gain and smallest coupling factor as expected by the reduction in mirror restoring force.

From devices (1,3,4) we can clearly see a trend in the mirror thickness. If it is too thick, it becomes stiff and losses stroke, but improves surface flatness and superposition holds. For space-based applications, device (3) is the best suitable in terms of gain, stability, coupling factor and general assumptions in high contrast imaging as superposition.

We verified that the device presented typical PZT hysteresis loop, when applied a cyclic voltage. This implies the presence of a small quadratic component, but we can assume that the stroke is mostly linear with voltage. The gain is $\approx$17 nm/V which is within space-based applications if we include the restrictions in the electronics.

For the ASIC, the electrical characterization shows control resolution of 0.04mV (20-bit), off leakage current of <4pA. Off leakage current at hold state off <2pA (1nF load) and static power dissipation of <4mW over the entire 20mm x 20mm ASIC. In future work, we will scale up the DM to 32x32 and 64x64, test different formats of DM-ASIC integrated systems, and carry on radiation hardness of the assembly.

ACKNOWLEDGMENTS

This work was performed at the Jet Propulsion Laboratory, California Institute of Technology, under contrast with the National Aeronautics and Space Adminsitration.

REFERENCES

[1] E. Cady, C. Mejia Prada, X. An, K. Balasubramanian, R. Diaz, N. J. Kasdin, B. Kern, A. Kuhnert, B. Nemati, I. Poberezhskiy, A. J. E. Riggs, R. Zimmer, and N. Zimmerman, "Demonstration of high contrast with an obscured aperture with the WFIRST-AFTA shaped pupil coronagraph," Journal of Astronomical Telescopes, Instruments, and Systems Special Section, SPIE 2(1), p. 011004, 2015.

[2] B.-J. Seo, B. Gordon, B. Kern, A. Kuhnert, D. Moody, R. Muller, I. Poberezhskiy, J. Trauger, and D. Wilson, "Hybrid Lyot Coronagraph for WFIRST-AFTA: Occulter Fabrication and High Contrast Narrowband Testbed Demonstration," Journal of Astronomical Telescopes, Instruments, and Systems Special Section, SPIE , 2015.

[3] N. Jovanovic et. al., "The Subaru Coronagraphic Extreme Adaptive Optics System: Enabling High-Contrast Imaging on Solar-System Scales", Publications of the Astronomical Society of the Pacific,127,955, 2015

[4] F. Zhao, "WFIRST-AFTA Coronagraph Instrument Overview", Proc. SPIE, 9143, 91430O, 2014.

[5] Exoplanet Exploration Program Technology Plan Appendix 2017, pp34-35

[6] W. Xingtao et. al.,"Driver ASICs for Deformable Mirrors," Imaging and Applied Optics, AOTh2C, 2015.

[7] G. Hickey, M. Ealey, and D. Redding, "Actuated hybrid mirrors for space telescopes", Proc.SPIE 7731, 773120, 2010

[8] J. Steeves et. al., "Multilayer active shell mirrors for space telescopes", Proc. SPIE, 9912, 99121K, 2016

[9] M. Bolcar et al., "Initial technology assessment for the Large-Aperture UV-Optical-Infrared (LUVOIR) mission concept study", Proc. SPIE, 9904, 99040J, 2016

Downloaded From: https://www.spiedigitallibrary.org/conference-proceedings-of-spie on 10/6/2017 Terms of Use: https://spiedigitallibrary.spie.org/ss/TermsOfUse.aspx